J. Phys. Earth, **43**, 117–130, 1995

Time Series Analysis of Groundwater Radon Using Stochastic Differential Equations

Tomoyuki Higuchi,[1] George Igarashi,[2,*] Yasunori Tohjima,[2] and Hiroshi Wakita[2]

[1] The Institute of Statistical Mathematics, Minato-ku, Tokyo 106, Japan
[2] Faculty of Science, The University of Tokyo, Bunkyo-ku, Tokyo 113, Japan

This paper provides a new approach to detect changes in the groundwater radon concentration related to an earthquake. We express changes in radon concentration in a radon-detection chamber by using stochastic linear differential equations. These equations are represented by the state space notation, and then its solution is replaced by an estimation of the state vector at discrete points in time with an assumption that the coefficients describing the stochastic differential equations are constant for a sufficiently small time interval. Since the solubility of radon in water depends strongly on temperature, the separation of radon from liquid water, which is necessary for radon detection, causes fluctuations in the observed radon concentrations due to water temperature changes in the chamber. We applied our procedure to some actual data sets on groundwater radon concentration with those on simultaneously observed water temperature, and found that the temperature effects on the fluctuations in the observed radon concentration can be satisfactorily described by our procedure. Furthermore, we were able to estimate the original radon concentration in groundwater before it was introduced into the radon-detection chamber, which was not affected by water temperature changes. The obtained original radon concentrations are very stable during normal periods, and anomalous changes associated with earthquakes were easily detected. Our new method will be very useful to examine time-variation patterns of changes in groundwater radon and will provide important information about the mechanism of radon changes related to earthquakes.

1. Introduction

Recently, reports on earthquake-related changes in groundwater radon, including preseismic and coseismic, have increased (e.g., Wakita *et al.*, 1989, 1991; Igarashi and Wakita, 1990; Igarashi *et al.*, 1993). It is now certain that the correlation between groundwater radon changes and earthquake occurrences is statistically significant. However, it is still poorly understood what mechanisms lead to changes in groundwater radon before and at the time of earthquakes. More detailed examinations of radon

Received October 11, 1994; Accepted May 10, 1995

* To whom correspondence should be addressed. Present address: Faculty of Science, Hiroshima University, Higashi-Hiroshima 724, Japan

changes such as time-variation patterns may provide important information about the mechanisms of radon changes related to earthquakes.

Continuous measurements of groundwater radon are usually carried out by introducing groundwater into a radon-detection chamber, where separation of radon gases from liquid water occurs. Then, the radon concentration in the gas phase of the chamber is measured by an α-ray detector mounted at the top (e.g., Noguchi and Wakita, 1977). Because the degassing flux of radon from liquid water depends on temperature, the measured radon concentration can fluctuate due to temperature changes even if the original radon concentration in groundwater remains constant. Furthermore, the time required to replace radon atoms in the radon-detection chamber with those degassed from newly introduced groundwater should be taken into account since this may result in a time delay between the observed radon changes and those in the original groundwater. Hence characteristics of a radon-detection system should carefully be evaluated before examining time-variation patterns of earthquake-related radon changes.

In this study, we express radon concentration changes in a radon-detection chamber by stochastic differential equations. We introduce the state-space notation (Kalman,1960; Jazwinski, 1970; Gelb, 1974; Anderson and Moore,1979) for solving these equations. Kalman (1960) advanced optimal recursive filter techniques based on the state-space formulation to estimate the state of the linear system. To measure the goodness of fit of the model to data, we adopt an information criterion which determines the optimal form for describing system and observation errors (Akaike, 1980; Gersch and Kitagawa, 1988). Then, by applying it to some observed radon data, we attempted to examine precisely the temperature effect and time delay in the measured radon concentrations, and to estimate time-variation patterns of original radon concentrations in groundwater before it is introduced into the radon-detection chamber.

2. Stochastic Differential Equations

We consider a radon-detection chamber whose inside consists of two homogeneous phases, gas and liquid phases. Figure 1 is a schematic figure of the chamber developed by Noguchi and Wakita (1977). Radon concentration changes in the chamber can be expressed by the following differential equations (Igarashi *et al.*, 1993),

$$V_g \frac{dC_g}{dt} = -\lambda V_g C_g + FS \tag{1}$$

$$V_l \frac{dC_l}{dt} = -\lambda V_l C_l - FS - QC_l + QC_0 . \tag{2}$$

Table 1 gives the notation for these equations. Since an α-ray detector is mounted at the top of the gas phase, what we can observe as radon concentration is C_g. We do not have direct observational data on C_l and C_0.

According to Liss and Slater (1974), gas exchange through the boundary between the gas and liquid phases is controlled by a very thin liquid surface layer where material movement is subject to molecular diffusion, and gas flux from the liquid phase can be approximated as

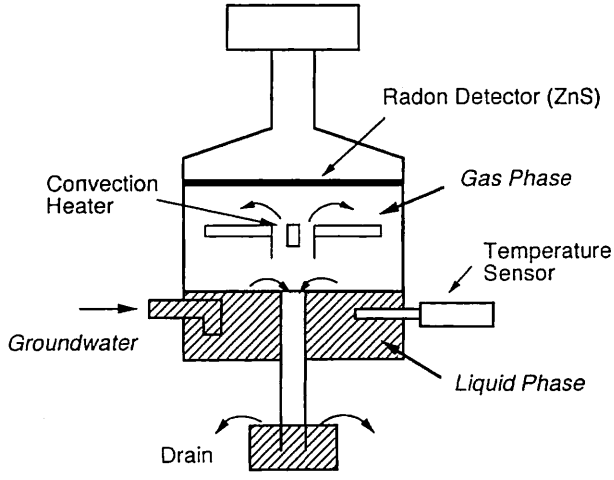

Fig. 1. Schematic figure of a radon-detection chamber.

Table 1. Notation for describing groundwater radon monitoring system.

		Values for the KSM station
C_g	Radon concentration in the gas phase	
C_l	Radon concentration in the liquid phase	
C_0	Original radon concentration in groundwater	
F	Radon flux through the phase boundary	
H_{Rn}	Henry's low constant of radon solubility in water	
Q	Flow rate of groundwater	$24\,cm^3/min$
S	Area of the phase boundary	$3.14\times10^2\,cm^3$
T_l	Temperature in the liquid phase	
V_g	Volume of the gas phase	$1.57\times10^3\,cm^3$
V_l	Volume of the liquid phase	$1.57\times10^2\,cm^3$
k_l	Gas exchange constant	0.086 cm/min*
λ	Decay constant of ^{222}Rn	1.26×10^{-4}/min

* The optimal value estimated by minimizing *AIC*.

$$F=k_l(C_l-C_g/H_{Rn})\,, \tag{3}$$

where k_l is a gas exchange constant for the liquid phase and H_{Rn} is the Henry's law constant of solubility of radon in water ($H_{Rn}=C_g/C_l$ in an equilibrium state). Although there are some empirical estimates of gas exchange constants appropriate for the sea surface (Liss and Slater, 1974), it is not certain whether we can apply those empirical estimates to the radon measuring system. Therefore, we will use an empirical estimate of k_l (0.144 cm/min for ^{222}Rn) as an initial value and will estimate the optimal value of k_l. The Henry's law constant H_{Rn} is a function of temperature. To calculate H_{Rn} from observed values of water temperature in the chamber (T_l[°C]), we use the following formulation,

$$H_{Rn}(T_l)^{-1}=0.50774-2.836\times10^{-2}T_l+4.683\times10^{-4}T_l-4.058\times10^{-6}T_l\,, \tag{4}$$

which we determined from the data tabulated in Wilhelm *et al.* (1976).

Putting Eq. (3) to Eqs. (1) and (2), the differential equations for describing the physics of our problem are rewritten as

$$\frac{dC_g}{dt} = aC_g + bC_l \tag{5}$$

$$\frac{dC_l}{dt} = dC_g + eC_l + fC_0 , \tag{6}$$

where

$$a = -\left(\lambda + \frac{k_l S}{H_{Rn} V_g}\right), \qquad b = \frac{k_l S}{V_g},$$

$$d = \frac{k_l S}{H_{Rn} V_l}, \qquad e = -\left(\lambda + \frac{Q}{V_l} + \frac{k_l S}{V_l}\right), \qquad f = \frac{Q}{V_l}. \tag{7}$$

In these equations, C_0 represents the system random disturbances. Although we can consider a number of models for system disturbances, we here assume that C_0 is represented by a random walk process. Accordingly, its system dynamic (differential) equation is given by

$$\frac{dC_0}{dt} = w_t , \tag{8}$$

where w_t is the scaler white noise with the autocorrelation function of $E[w_t w_{t'}] = \tau^2 \delta(t-t')$. $E[\cdot]$ denotes the operation of an expectation, an $\delta(t)$ is the Dirac delta function.

3. State Space Representation

We here introduce the state-space notation which offers the advantage of mathematical and notational convenience for solving the system dynamic (i.e., vector-matrix differential) equation (Gelb, 1974). We define the state vector at time t to be $\boldsymbol{x}_t = [C_g, C_l, C_0]^T$, where T denotes a transposition. The first-order linear, lumped differential Eqs. (5), (6), and (8) are represented by the first-order vector-matrix differential equation

$$\frac{d\boldsymbol{x}_t}{dt} = F_t \boldsymbol{x}_t + G_t w_t , \tag{9}$$

where F_t is the system dynamic matrix defined by

$$F_t = \begin{bmatrix} a & b & 0 \\ d & e & f \\ 0 & 0 & 0 \end{bmatrix} \tag{10}$$

and G_t is the time-independent matrix defined by $G_t = G = [0, 0, 1]^T$. In other words, the rate of change of the state vector consists of two terms. The first, $F_t x_t$, would be a deterministic rate of change if F_t were known. The system dynamic matrix F_t is considered to vary with temperature. The second term is random noise.

The first step for solution of the system dynamic equation is to get the transition matrix which allows calculation of the state vector at some time $t = t_1$, given knowledge of the state vector at $t = t_0$, in the absence of w_t. When the matrix F_t is time-invariant, the transition matrix, $\Phi(t_1, t_0)$, is determined by

$$\Phi(t_1, t_0) = e^{F_t(t_1 - t_0)} . \tag{11}$$

In our case, when the temperature can be assumed to be constant during a small interval between t_0 and t_1, F_t becomes the time-invariant during this interval. Hereafter we, explicitly indicate this time-invariant matrix F_t between t_0 and t_1 by F_{t_1}. Derivation of $\Phi(t_1, t_0)$ is given in Appendix A.

The obtained transition matrix yields the solution of the dynamic equation of Eq. (9) given by

$$x_{t_1} = \Phi(t_1, t_0) x_{t_0} + \int_{t_0}^{t_1} \Phi(t_1, s) G w_s \mathrm{d}s = \Phi_{t_1}(\Delta t) x_{t_0} + \int_0^{\Delta t} \Phi_{t_1}(\xi) G w_{t_1 - \xi} \mathrm{d}\xi . \tag{12}$$

This representation provides the discrete state space representation

$$\begin{aligned} x_{t_1} &= \Phi_{t_1}(\Delta t) x_{t_0} + u_{t_1, t_0} \\ y_{t_1} &= H x_{t_1} + v_{t_1} , \end{aligned} \tag{13}$$

where

$$\begin{aligned} u_{t_1, t_0} &= \int_0^{\Delta t} \Phi_{t_1}(\xi) G w_{t_1}(\xi) G w_{t_1 - \xi} \mathrm{d}\xi \\ H &= [1, 0, 0] . \end{aligned} \tag{14}$$

u_{t_1, t_0} and v_{t_1} are called the system noise and observation noise, respectively. y_{t_1} is an observation at time $t = t_1$.

The (i, j) element of the variance and covariance matrix of u_{t_1, t_0}, designated $Q^{i,j}_{t_1, t_0}$, is determined by calculating $E[u^i_{t_1, t_0} \cdot u^j_{t_1, t_0}]$, where $u^i_{t_1, t_0}$ is the i-th component of the vector u_{t_1, t_0}. Derivation of $Q^{i,j}_{t_1, t_0}$ is given in Appendix B.

4. Estimation of the State Vector

The measurements in this study are taken with the equal sampling interval Δt, and then we denote the state vector and observation at time $t = t_n$, x_{t_n} and y_{t_n}, by x_n and y_n, respectively. Thus, the observation in our problem is designated by $Y_N = [y_1, \cdots, y_N]$, where N is the total data number. Similarly, the observation of temperature in the liquid phase at time $t = t_n$ is specified by $T_{l,n}$. Since there is no need to explicitly indicate a dependency on the interval Δt for $\Phi_{t_1}(\Delta t)$ and $Q_{t_1}(\Delta t, \tau^2)$, we denote them by Φ_n and $Q_n(\tau^2)$, respectively. By this notation, the state space representation given by Eq. (13) can be rewritten as

$$\boldsymbol{x}_n = \boldsymbol{\Phi}_n \boldsymbol{x}_{n-1} + \boldsymbol{u}_n$$
$$y_n = H\boldsymbol{x}_n + v_n \,, \tag{15}$$

where $\boldsymbol{u}_n$ corresponds to $\boldsymbol{u}_{t_n, t_{n-1}}$. Of course, the variance and covariance matrix of $\boldsymbol{u}_n$ is $Q_n(\tau^2)$. This representation enables us to use an efficient computation algorithm for estimating the state vector, namely the following Kalman filter algorithm (Anderson, 1979; Kitagawa, 1983; Gersch and Kitagawa, 1988; Higuchi, 1991).
prediction

$$\boldsymbol{x}_{n|n-1} = \boldsymbol{\Phi}_n \boldsymbol{x}_{n-1|n-1}$$
$$V_{n|n-1} = \boldsymbol{\Phi}_n V_{n-1|n-1} \boldsymbol{\Phi}_n^{\mathrm{T}} + Q_n(\tau^2) \tag{16}$$

filtering

$$K_n = V_{n|n-1} H^{\mathrm{T}} (H V_{n|n-1} H^{\mathrm{T}} + 1)^{-1}$$
$$\boldsymbol{x}_{n|n} = \boldsymbol{x}_{n|n-1} + K_n (y_n - H\boldsymbol{x}_{n|n-1})$$
$$V_{n|n} = (I - K_n H) V_{n|n-1} \,, \tag{17}$$

where $\boldsymbol{x}_{n|n-1}$ and $\boldsymbol{x}_{n|n}$ denote the estimates of $\boldsymbol{x}_n$ given the observations $Y_{n-1} = [y_1, \cdots, y_{n-1}]$ and $Y_n = [y_1, \cdots, y_{n-1}, y_n]$, respectively. Similarly, $V_{n|n-1}$ and $V_{n|n}$ stand for their corresponding estimation error covariances. The estimates of $\boldsymbol{x}_n$ and V_n based on all the available information $Y_N = [y_1, \cdots, y_N]$, $\boldsymbol{x}_{n|N}$ and $V_{n|N}$, are also obtained by the following recursive algorithm:
fixed-interval smoothing

$$A_n = V_{n|n} \boldsymbol{\Phi}_n^{\mathrm{T}} V_{n+1|n}^{-1}$$
$$\boldsymbol{x}_{n|N} = \boldsymbol{x}_{n|n} + A_n (\boldsymbol{x}_{n+1|N} - \boldsymbol{x}_{n+1|n})$$
$$V_{n|N} = V_{n|n} + A_n (V_{n+1|N} - V_{n+1|n}) A_n^{\mathrm{T}} \,. \tag{18}$$

The optimal value for τ^2 is easily identified by evaluating the following log-likelihood,

$$l(Y_N | \tau^2, \sigma^2) = \log P(y_1) + \sum_{n=2}^{N} \log P(y_n | Y_{n-1}) \tag{19}$$

with

$$P(y_n | Y_{n-1}) = \frac{1}{\sqrt{2\pi\sigma^2 v_n}} \exp\left(-\frac{\varepsilon_n^2}{2\sigma^2 v_n} \right),$$
$$v_n = H V_{n|n-1} H^{\mathrm{T}} + 1 \,,$$
$$\varepsilon_n = y_n - H\boldsymbol{x}_{n|n-1} \,. \tag{20}$$

It is interesting to note that both v_n and ε_n appear in Eq. (17). σ^2 is the variance of the observation noise v_n and its estimate is given by

$$\hat{\sigma}^2 = \frac{1}{N} \sum_{n=1}^{N} \frac{\varepsilon_n^2}{v_n} \tag{21}$$

by maximizing Eq. (19). By inserting Eq. (21) into Eq. (20), the log-likelihood of the hyper-parameter τ^2 can be expressed as

$$l(Y_N|\tau^2) = -\frac{N}{2}(\log 2\pi\hat{\sigma}^2 + 1) - \frac{1}{2} \sum_{n=1}^{N} \log v_n . \tag{22}$$

We can obtain the optimal τ^2 by maximizing Eq. (22) or by minimizing the Akaike (Bayesian) information Criterion, called *AIC*,

$$AIC = -2 \max l(Y_N|\tau^2) + 2 \text{ (number of hyper-parameters)} \tag{23}$$

with respect to τ^2. When there exists uncertainty about the initial given value of any constant, we can correct its estimate by treating it as a hyper-parameter and minimizing Eq. (23). As mentioned in Sec. 2, we do not have a reliable estimate for the gas exchange constant k_1 in Eq. (3); we will determine an optimal value of k_1 by minimizing *AIC* with respect to k_1.

The nonlinear optimization for determining the hyper-parameter is performed in this study by using the Broydon-Fletcher-Goldfarb-Shanno (BFGS) algorithm to implement the quasi-Newton methods (e.g., Press *et al.*, 1988). The state vector obtained by the smoothing algorithm, $x_{n|N}$, at the value of hyper-parameter maximizing Eq. (23) is specified by $\hat{x}_n$. Correspondingly, the estimators for C_g, C_1, and C_0, are denoted by $\hat{C}_g$, $\hat{C}_1$, and $\hat{C}_0$.

In the actual computation shown above, the initial state vector and variance-covariance matrix, $x_{0|0}$ and $Q_{0|0}$, are required and given in this study by the backward Kalman filtering. The initial estimate of C_g in the process of the backward Kalman filtering is set to y_N. Other initial estimates for x_n, C_1, and C_0, are determined by setting d/dt in Eqs. (5) and (6) to zero. The initial estimate for Q_n, $Q_{0|0}$, is simply set to the diagonal matrix with equal large diagonal values such as 10^6.

5. Results and Discussion

We applied our method to actual radon concentration data obtained at a monitoring station named KSM, which is located in northeast Japan. A detailed description of the station can be found elsewhere (Igarashi and Wakita, 1990). The instrument for radon monitoring is NW101 Aqua Radon Meter (Aloca Co.); some values about the size of the radon-detection chamber are listed in Table 1. The observation well is a 200-m deep artesian well of 10 cm in diameter. A strainer is positioned at a depth from 124 to 129 m. The groundwater, welling up with a flow rate of about 24 cm^3/min, is introduced into the radon-detection chamber. The observed radon concentration (C_{obs}) at the KSM station is shown in Fig. 2(e) for the period from January 1 to March 31, 1987. Because of the small groundwater flow rate, the temperature of the water is easily affected by environmental temperature changes. The temperature in the radon-detection chamber is monitored together with the radon concentration as shown in Fig. 2(d).

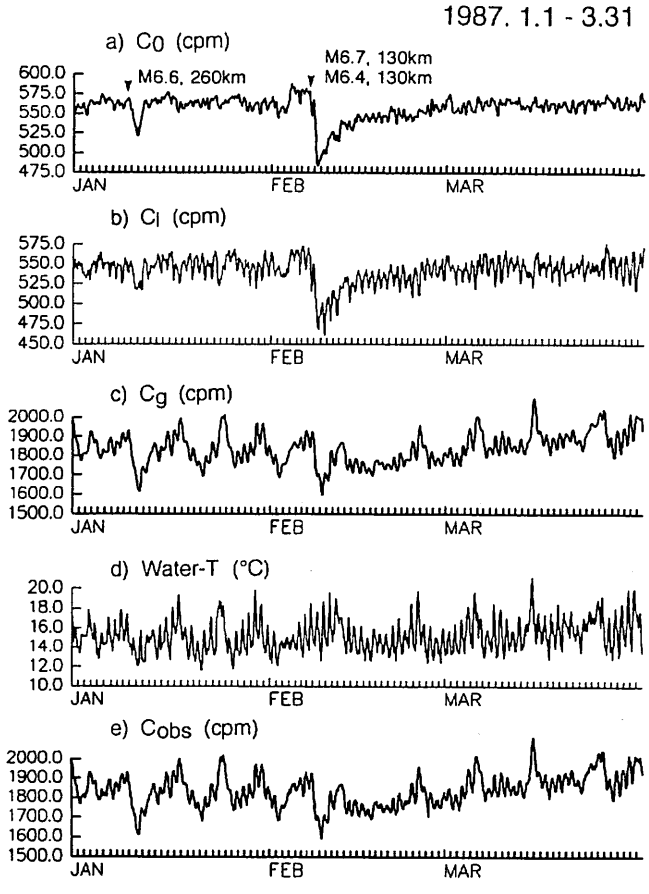

Fig. 2. An example of the analytical results and observed data for the period from January 1 to March 31, 1987: estimated values of, (a) original, (b) liquid phase, and (c) gas phase radon concentrations, and observed values of, (d) water temperature and (e) radon concentration. The data were taken at the KSM station, northeast Japan (Igarashi and Wakita, 1990). Radon concentrations are expressed as cpm (count per minute). Major earthquakes are shown with their magnitudes (reported by Japan Meteorological Agency) and hypocentral distances from the KSM station.

The measurements of y_n (C_{obs}) and $T_{\text{l},n}$ (Water-T) are taken hourly, and in our case this leads to a poor assumption for temperature invariance during the sampling interval. As a result, the transition matrix Φ_n defined by $T_{\text{l},n}$ is inappropriate for the transition matrix applied throughout the interval t_{n-1} and t_n. To deal with this problem, we generate the minutely temperature data by linearly interpolating an original time series, $T_{\text{l},n}$. Namely, we make a minute data $\tilde{T}_m$ ($m=1, \cdots, 60 \times N$) from $T_{\text{l},n}$ ($n=1, \cdots, N$). This manipulation is quite natural, because the dependency of temperature on time is definitely gradual in our problem and then the temperature in the liquid phase during a minute can be satisfactorily approximated to be constant.

Correspondingly, we make a new time series $\tilde{y}_m$ ($m=1, \cdots, 60 \times N$) from the hourly data y_n. It should be noted that we do not have to interpolate y_n, and we simply

treat $\tilde{y}_m$ for Mod$(m, 60) \neq 0$ as a missing value. Consequently, we apply the procedure for estimating the state vector, explained in Sec. 4, to these newly generated time series $(\tilde{y}_m, \tilde{T}_m)$ $(m=1, \cdots, 60 \times N)$.

In Fig. 2(a), (b), and (c), we show the solution of the maximum AIC with respect to hyper-parameters τ and k_1. The obtained optimum values of the hyper-parameters are $\hat{\tau}^2 = 5.64 \times 10^{-3}$ and $\hat{k}_1 = 0.086$ cm/min. The value of $\hat{k}_1$ is about 40% smaller than the initial value that is estimated from measurements of gas exchange through the air-sea interface. It is interesting that the gas exchange constant estimated for the radon-detection chamber is within a factor of two of that for the sea surface.

Since $\hat{\sigma}^2$ with the minimum AIC is very small, the estimated $\hat{C}_g$ is almost identical to the observed radon concentration C_{obs}. It is easily recognized that a large part of the fluctuations in $\hat{C}_g (\simeq C_{obs})$ is caused by changes in temperature in the chamber. Complementary fluctuations can be seen in $\hat{C}_1$. As a result, the original radon concentration $\hat{C}_0$ was estimated to be nearly constant, except for two changes associated with earthquakes. The amplitude of random fluctuations remaining in $\hat{C}_0$ is characterized by the hyper-parameter τ. A standard deviation of $\hat{C}_0$ from March 1 to 31, when no earthquake-related change was observed, is about 1% of the average concentration. Statistical errors in counting α particles, which correspond to the square roots of the total counts every hour, are also about 1%; that is, it is impossible to reduce the background fluctuations to less than 1%. Hence, we have succeeded in estimating the original radon concentrations in groundwater to a level of precision equal to that of the instrument's ability.

Characteristic time constants of response of $\hat{C}_g$ and $\hat{C}_1$ to changes in temperature and $\hat{C}_0$ can be expressed by reciprocals of the eigen values of the matrix F_{t_1}, i.e., ω_1^{-1} and ω_2^{-1} (Appendix A). Putting the value of $\hat{k}_1$ and other constants, we obtain $\omega_1^{-1} \simeq 5$ h and $\omega_2^{-1} \simeq 2$ min. The large value of ω_1^{-1} can be attributed mainly to the small k_1 and large V_g. Thus, it is expected that there exists a significant time delay in the response of $\hat{C}_g$ to changes in temperature and $\hat{C}_0$. Figure 3 is a close-up of the estimated values of radon concentrations in the chamber ($\hat{C}_0$, $\hat{C}_g$, $\hat{C}_1$), and the observed values of radon concentration (C_{obs}) and water temperature (Water-T), when the most remarkable post-seismic change occurred. It can be seen that daily variations in C_{obs} lag behind the temperature variations by several hours. Furthermore, it should be noted that the post-seismic decrease detected in the estimated $\hat{C}_0$ started several hours earlier than the apparent decrease in C_{obs}. In fact, a correlation coefficient between $\hat{C}_0$ and C_{obs} becomes largest when a time lag of 5 h is assumed. Thus, our method appears to be very useful for closer examination of the characteristics of actual changes in the original groundwater, which will provide important information about the mechanism of radon changes caused by earthquakes.

6. Conclusions

By applying our new method of time series analysis to an actual data set on groundwater radon concentration obtained at the KSM station, northeast Japan, we have drawn the following conclusions concerning the characteristics of the radon

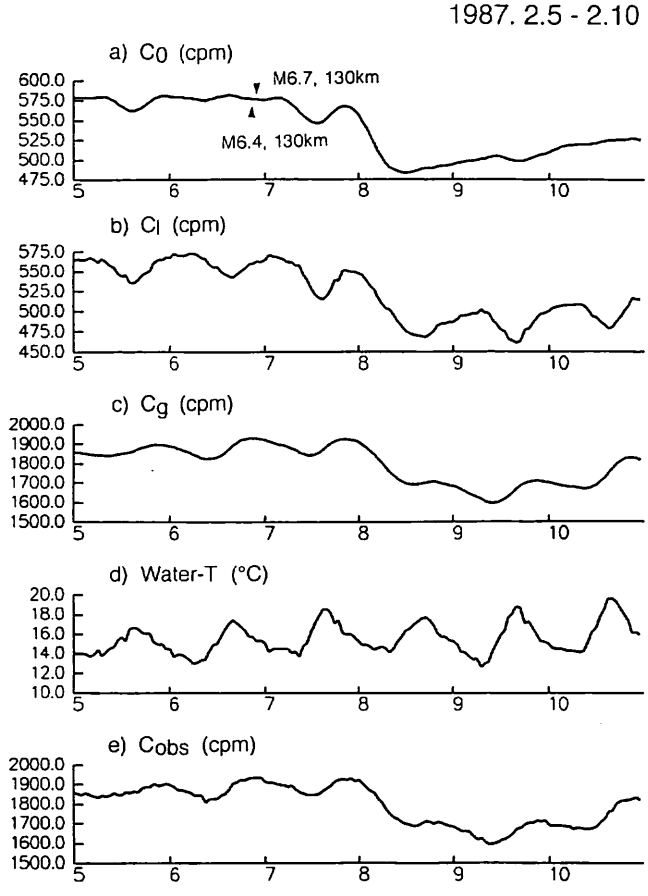

Fig. 3. A close-up of an earthquake-related radon change (February 5 to 10, 1987): estimated values of, (a) original, (b) liquid phase, and (c) gas phase radon concentrations, and observed values of, (d) water temperature and (e) radon concentration.

measuring system and the relationship between the observed and original radon concentration of groundwater.

Most of the fluctuations in the radon concentration observed at the KSM station can be explained by changes in radon flux through the interface between the gas and liquid phases in the radon-detection chamber, which is caused by temperature changes. The exchange constant of radon through the interface was determined to be $k_l = 0.086$ cm/min, which is within a factor of two of that estimated for the sea surface (Liss and Slater, 1974).

Fluctuations in the estimated value of the original radon concentration in groundwater is about 1% of the average value, which is as small as the statistical error of α-ray counting. Thus, the original radon concentration in a normal condition can be regarded as constant within the instrumental uncertainty. Anomalous radon changes associated with earthquakes can be clearly identified in the estimated original radon concentration. There is a time delay of about 5 h in the response of the observed radon concentration to changes both in temperature and the original radon concentration, which can be attributed to the small value of radon flux through the interface between

gas and liquid phases in the radon-detection chamber.

We thank two anonymous reviewers for comments and suggestions. This work was supported by the Ministry of Education, Science and Culture, Japan, under Grant-in-Aid for Encouragement of Young Scientists 06780220, and partly carried out under the ISM cooperative Research Program (94-ISM. CRP-5).

REFERENCES

Akaike, H., Likelihood and the Bayes procedure (with discussion), in *Bayesian Statistics*, ed. J. M. Bernardo, M. H. De Groot, D. V. Lindley, and A. F. M. Smith, pp. 143–166, University Press, Valencia, 1980.

Anderson, B. D. O. and J. B. Moore, *Optimal Filtering*, Prentice-Hall, Englewood Cliffs, N.J., 1979.

Gelb, A., *Applied Optimal Estimation*, M.I.T. Press, Massachusetts, 1974.

Gersch, W. and G. Kitagawa, Smoothness priors in time series, in *Bayesian Analysis of Time Series and Dynamic Models*, ed. J. C. Spall, pp. 431–476, Marcel Dekker, Inc., New York and Basel, 1988.

Higuchi, T., Method to subtract an effect of the geocorona EUV radiation from the low energy particle (LEP) data by the Akebono (EXOS-D) Satellite, *J. Geomag. Geoelectr.*, **43**, 957–978, 1991.

Igarashi, G. and H. Wakita, Groundwater radon anomalies associated with earthquakes, *Tectonophysics*, **180**, 237–254, 1990.

Igarashi, G., Y. Tohjima, and H. Wakita, Time-variable response characteristics of groundwater radon, *Geophys. Res. Lett.*, **20**, 1807–1810, 1993.

Jazwinski, J. Z., *Stochastic Processes and Filtering Theory*, Academic Press, New York, 1970.

Kalman, R. E., A new approach to linear filtering and prediction problems, *Trans. ASME, J. Basic Eng.*, **82D**, 35–45, 1960.

Kitagawa, G., Changing spectrum estimation, *J. Sound Vib.*, **89**, 433–445, 1983.

Liss, P. S. and P. G. Slater, Flux of gases across the air-sea interface, *Nature*, **247**, 181–184, 1974.

Noguchi, M. and H. Wakita, a method for continuous measurement of radon in groundwater for earthquake prediction, *J. Geophys. Res.*, **82**, 1353–1357, 1977.

Press, W. H., B. P. Flannery, S. A. Teukolsky and W. T. Vetterling, *Numerical Recipes in FORTRAN*, Cambridge University Press, Cambridge, 1988.

Wakita, H., G. Igarashi, and K. Notsu, An anomalous radon decrease in groundwater prior to an *M*6.0 earthquake: a possible precursor?, *Geophys. Res. Lett.*, **16**, 417–420, 1989.

Wakita, H., G. Igarashi, Y. Nakamura, Y. Sano, and K. Notsu, Coseismic radon changes in groundwater, *Geophys. Res. Lett.*, **18**, 629–632, 1991.

Wilhelm, E., R. Battino, and R. J. Wilcock, Low-pressure solubility of gases in liquid water, *Chem. Rev.*, **77**, 219–262, 1976.

APPENDIX

A. Derivation of the Transition Matrix $\Phi(t_1, t_0)$

Suppose we transform the matrix F_{t_1} according to $J_{t_1} = U_{t_1}^{-1} F_{t_1} U_{t_1}$, for some

transformation matrix U_{t_1}. Accordingly, the exponential $e^{F t_1}$ is determined through the following useful relation

$$e^{F_{t_1}(t_1-t_0)}=e^{U_{t_1}J_{t_1}U_{t_1}^{-1}(t_1-t_0)}=U_{t_1}e^{J_{t_1}(t_1-t_0)}U_{t_1}^{-1}. \tag{A1}$$

If we are able to calculate matrix $e^{J_{t_1}(t_1-t_0)}$ analytically, an analytic form of $e^{F_{t_1}(t_1-t_0)}$ is easily obtained through Eq. (A1).

Although the matrix F_{t_1} is singular, we can find the matrix J_{t_1} with a convenient form,

$$J_{t_1}=\begin{bmatrix} \omega_1 & 0 & f/\rho \\ 0 & \omega_2 & -f/\rho \\ 0 & 0 & 0 \end{bmatrix}, \tag{A2}$$

with the transformation matrix U_{t_1},

$$U_{t_1}=\begin{bmatrix} b & b & 0 \\ \omega_1-a & \omega_2-a & 0 \\ 0 & 0 & 1 \end{bmatrix}, \tag{A3}$$

where ω_i $(i=1, 2, 3)$ as the eigen values of the matrix F_{t_1} and given by

$$\omega_1=\frac{a+e+\sqrt{(a-e)^2+4bd}}{2}$$

$$\omega_2=\frac{a+e-\sqrt{(a-e)^2+4bd}}{2}$$

$$\omega_3=0, \tag{A4}$$

and ρ is $\omega_1-\omega_2=\sqrt{(a-e)^2+4bd}$. It should be reminded that both ω_1 and ω_2 are real for any F_t in our case and that there is no equal root. Here, for the following convenient notation, we set $\Omega_1=\omega_1-a$ and $\Omega_2=\omega_2-a$. Then, the inverse matrix of U_{t_1} is

$$U_{t_1}^{-1}=\begin{bmatrix} -\Omega_2/(b\rho) & 1/\rho & 0 \\ \Omega_1/(b\rho) & -1/\rho & 0 \\ 0 & 0 & 1 \end{bmatrix}, \tag{A5}$$

To get the matrix exponential $e^{J_{t_1}}$, we compute the J_{t_1} power to n and get

$$J_{t_1}^n=\begin{bmatrix} \omega_{t_1}^n & 0 & f\omega_1^{n-1}/\rho \\ 0 & \omega_2^n & -f\omega_2^{n-1}/\rho \\ 0 & 0 & 0 \end{bmatrix}, \tag{A6}$$

Hence, by using the matrix exponential series expansion

$$e^{J_{t_1}(t_1-t_0)}=I+J_{t_1}(t_1-t_0)+\frac{1}{2!}J_{t_1}^2(t_1-t_0)^2+\cdots+\frac{1}{n!}J_{t_1}^n(t_1-t_0)^n+\cdots, \tag{A7}$$

$e^{J_{t_1}(t_1-t_0)}$ is written as

$$e^{J_{t_1}(t_1-t_0)}=\begin{bmatrix} e^{\omega_1(t_1-t_0)} & 0 & f(e^{\omega_1(t_1-t_0)}-1)/(\omega_1\rho) \\ 0 & e^{\omega_2(t_1-t_0)} & -f(e^{\omega_2(t_1-t_0)}-1)/(\omega_2\rho) \\ 0 & 0 & 1 \end{bmatrix}. \tag{A8}$$

Since the transition matrix depends only on the interval t_1-t_0 as a function of time, we then set $\Delta t=t_1-t_0$ and specify $\Phi(t_1, t_0)$ by $\Phi_{t_1}(\Delta t)$. It should be noted that the subscript of $\Phi_{t_1}(\Delta t)$, t_1, explicitly indicates that the transition matrix is defined by using F_{t_1}. According to Eq. (A1), we get the transition matrix $\Phi_{t_1}(\Delta t)$,

$$\Phi(t_1, t_0)=\Phi_{t_1}(\Delta t)=U_{t_1}e^{J_{t_1}\Delta t}U_{t_1}^{-1}=\begin{bmatrix} (\Omega_1 e^{\omega_2\Delta t}-\Omega_2 e^{\omega_1\Delta t})/\rho & b/\rho\cdot(e^{\omega_1\Delta t}-e^{\omega_2\Delta t}) \\ \Omega_1\Omega_2(e^{\omega_2\Delta t}-e^{\omega_1\Delta t})/(b\rho) & (\Omega_1 e^{\omega_1\Delta t}-\Omega_2 e^{\omega_2\Delta t})/\rho \\ 0 & 0 \end{bmatrix}$$
$$\begin{bmatrix} bf((e^{\omega_1\Delta t}/\omega_1-e^{\omega_2\Delta t}/\omega_2)/\rho+1/(\omega_1\omega_2)) \\ f/\rho\cdot((\Omega_1 e^{\omega_1\Delta t}/\omega_1-\Omega_2 e^{\omega_2\Delta t}/\omega_2)+(\Omega_2/\omega_2-\Omega_1/\omega_1)) \\ 1 \end{bmatrix}, \tag{A9}$$

B. Derivation of the Variance and Covariance Matrix $Q_{t_1,t_0}^{i,j}$

Before calculating $Q_{t_1,t_0}^{i,j}$, we rewrite u_{t_1,t_0}^{i} in the clear form as follows:

$$u_{t_1,t_0}^{i}=\int_0^{\Delta t}(p_i e^{\omega_1\xi}+q_i e^{\omega_2\xi}+r_i)w_{t_1-\xi}\,d\xi\,, \tag{B1}$$

where

$$\begin{aligned} &p_1=bf/(\omega_1\rho) && q_1=-bf/(\omega_2\rho) && r_1=bf/(\omega_1\omega_2) \\ &p_2=f\Omega_1/(\omega_1\rho) && q_2=-f\Omega_2/(\omega_2\rho) && r_2=f/\rho\cdot(\Omega_2/\omega_2-\Omega_1/\omega_1) \\ &p_3=0 && q_3=0 && r_3=1\,. \end{aligned} \tag{B2}$$

By this substitution, $E[u_{t_1,t_0}^{i}\cdot u_{t_1,t_0}^{j}]$ is rewritten as

$$E[u_{t_1,t_0}^{i}\cdot u_{t_1,t_0}^{j}]=E\left[\int_0^{\Delta t}\int_0^{\Delta t}(p_i e^{\omega_1\xi}+q_i e^{\omega_2\xi}+r_i)w_{t_1-\xi}(p_j e^{\omega_1\eta}+q_j e^{\omega_2\eta}+r_j)w_{t_1-\eta}\,d\xi d\eta\right]$$
$$=\int_0^{\Delta t}\int_0^{\Delta t}(p_i e^{\omega_1\xi}+q_i e^{\omega_2\xi}+r_i w_{t_1-\xi})(p_j e^{\omega_1\eta}+q_j e^{\omega_2\eta}+r_j w_{t_1-\eta})$$
$$\times E[w_{t_1-\xi}w_{t_1-\eta}]\,d\xi d\eta\,. \tag{B3}$$

By using the properties of the delta function, $E[w_t w_{t'}]=\tau^2\delta(t-t')$ mentioned in Sec. 2, we can perform this integration:

$$E[u_{t_1,t_0}^{i}\cdot u_{t_1,t_0}^{j}]=\tau^2\int_0^{\Delta t}\int_0^{\Delta t}(p_i e^{\omega_1\xi}+q_i e^{\omega_2\xi}+r_i)(p_j e^{\omega_1\eta}+q_j e^{\omega_2\eta}+r_j)\delta(\xi-\eta)\,d\xi d\eta$$

$$=\tau^2\int_0^{\Delta t}(p_i e^{\omega_1\xi}+q_i e^{\omega_2\xi}+r_i)(p_j e^{\omega_1\xi}+q_j e^{\omega_2\xi}+r_j)\,d\xi\,. \tag{B4}$$

Consequently, we obtain

$$Q^{i,j}_{t_1,t_0}(\tau^2)=\tau^2\left\{\frac{p_i p_j}{2\omega_1}(e^{2\omega_1\Delta t}-1)+\frac{q_i q_j}{2\omega_2}(e^{2\omega_2\Delta t}-1)+\frac{p_i q_j+q_i p_j}{\omega_1+\omega_2}(e^{(\omega_1+\omega_2)\Delta t}-1)\right.$$
$$\left.+\frac{p_i r_j+r_i p_j}{\omega_1}(e^{\omega_1\Delta t}-1)+\frac{q_i r_j+r_i q_j}{\omega_2}(e^{\omega_2\Delta t}-1)+r_i r_j\Delta t\right\}$$
$$(\text{for}\quad i=1,2,3\,,\quad j=1,2,3)\,. \tag{B5}$$

$Q_{t_1,t_0}(\tau^2)$ also depends only on the interval t_1-t_0 as a function of time, and henceforth we specify it by $Q_{t_1}(\Delta t,\tau^2)$.